

Active Acoustic Impedance Mapping using Mobile Robots

Yihui Feng, Reza Khodayi-mehr, Yiannis Kantaros, Luke Calkins, and Michael M. Zavlanos

Abstract—In this paper we address the problem of autonomous Impedance Mapping (IM) of an environment using a team of mobile robots. IM of a domain provides the boundary information required to model the sound propagation in the domain. We equip the robots with a speaker and two microphones and utilize the two-microphone reflection method to estimate the normal surface impedance of the boundaries. Specifically, while a speaker robot plays white noise, a listener robot measures the pressure values at two adjacent points next to the sample and uses this data to estimate its impedance. We model the collaborative IM task using Linear Temporal Logic and design motion plans that allow the robots to switch between speaker and listener roles while maintaining desired distances from each other and the samples, and measure the impedance of every boundary segment. We present experimental results and validate our impedance measurements by comparing to a standard method.

I. INTRODUCTION

Acoustic properties of materials such as the reflection coefficient, the surface impedance, and the absorption coefficient govern how these materials respond to sound waves and are of great importance for many applications. For instance, absorbent materials, e.g., glass wool, mineral wool, and porous foam, are often used to absorb sound in industrial and residential buildings [1]. Moreover, the acoustic properties of materials are essential for the solution of the acoustic wave equation which is the mathematical model for sound propagation [2]. Active Source Identification (ASI) is one particular application that relies on the solution of the wave equation [3]–[5]. In this problem, a team of mobile robots autonomously collect pressure measurements and solve an optimization problem subject to the wave equation to identify acoustic sources. In such scenarios, measuring the acoustical properties of the environment is critical and enabling the robots to autonomously measure these properties can facilitate the solution of the ASI problem. Moreover, since acoustic impedance depends on many problem-dependent factors including size, thickness, and structure among others, it is difficult to tabulate impedance values and in situ measurements are preferred. Thus, using autonomous robots to perform these impedance measurements can be very advantageous.

There exist different methods to measure the acoustic impedance of materials. Generally, these methods can be categorized into three types, reverberation room methods, tube methods, and reflection methods [6]. Reverberation room methods measure the diffuse incidence absorption coefficient as opposed to the normal incidence [7]. These methods require equipment that is expensive and bulky, making them unsuitable for in situ measuring. Moreover, measurements of the same

material depend on the type of the reverberation room and are affected by the position of the sample in the room. Finally, the results for high frequencies are inaccurate [8].

Tube methods are another set of conventional methods that are more cost effective and accurate. These methods can be categorized into two types, standing wave ratio methods [9] and transfer function methods [10], [11]. They require the sample to be cut precisely to fit in a tube which often causes inaccuracies due to the gap between the sample and the inner diameter of the tube. In addition, the absorption coefficient measured at the laboratory will not completely represent the true value which is problem-dependent.

Compared to reverberation room methods and tube methods, reflection methods provide a natural framework for in situ measurements. The authors in [6], [12] have developed some of the early methods of this type. These methods only require two microphones but are only accurate for low frequencies and the arrangement of speakers, microphones, and samples could be complex. In [13] a simpler method is developed that uses ambient noise instead of a speaker. Due to randomness in ambient noise, the results need to be averaged over time and are accurate for frequencies less than 1500Hz. In this paper, we adapt the method proposed in [13] and add a controlled sound source to minimize randomness. This results in more accurate estimations for a wider frequency range.

To the best of our knowledge, in situ measurement of acoustic impedance using mobile robots has not been considered in the literature. In this paper, we propose a first approach to Autonomous Impedance Mapping (AIM) that employs the two-microphone reflection method proposed in [13] executed by teams of mobile robots. Specifically, we equip every robot with a speaker and a pair of microphones. Each robot can act either as a speaker or listener. The microphones on a listener robot record the sound from a speaker robot. Then, the listener robot estimates the acoustic impedance of the sample using pressure phase information, where a sample is a boundary segment made of a single material. Since the pressure wave is assumed to be planar, the distance between the sample and the speaker has a lower bound, imposing constraints on the distance between speaker and listener robots and the samples. We model the AIM task using Linear Temporal Logic (LTL) specifications and employ optimal control synthesis algorithms [14]–[16] to design motion plans that allow the robots to switch between speaker and listener roles and measure the impedance of every sample in the domain, while maintaining desired distances from each other and the samples and minimizing a desired cost function, such as travel distance or energy consumption. The end goal is to measure the acoustic impedance at a discrete set of locations and to construct an Impedance Map (IM) of the domain of interest.

The contributions of this paper are as follows. To the best

Yihui Feng, Reza Khodayi-mehr, Yiannis Kantaros, Luke Calkins, and Michael M. Zavlanos are with the Department of Mechanical Engineering and Materials Science, Duke University, Durham, NC 27708, USA, {yihui.feng, reza.khodayi.mehr, yiannis.kantaros, william.calkins, michael.zavlanos}@duke.edu.

of our knowledge, this is the first paper to address the problem of AIM using a team of mobile robots. We design the mobile robot that carries out this task and optimize its structure to minimize acoustic interference caused by the presence of the robots. Moreover, we formulate the proposed planning problem by a global LTL formula and solve the resulting problem. We demonstrate the performance of our method in experiments and examine the accuracy of our in situ impedance estimates by comparing to a benchmark approach using a tube method.

The remainder of this paper is organized as follows. In Section II we discuss the details of the method used to estimate the impedance. Section III is devoted to the formulation of the planning problem for the team of robots. We present our experimental results in Section IV and finally, Section V concludes the paper.

II. TWO-MICROPHONE REFLECTION METHOD

The acoustic wave equation models the pressure field \hat{p} as a function of the temporal and spatial coordinates given a set of Boundary Conditions (BCs) and an acoustic source \hat{s} as

$$\nabla^2 \hat{p} - \frac{1}{c^2} \frac{\partial^2 \hat{p}}{\partial t^2} = \hat{s},$$

where c is the sound speed in the desired medium. Three types of BCs are often specified for this equation, acoustic pressure, velocity, and impedance conditions. The latter is defined as the ratio of acoustic pressure to acoustic velocity and is the most general form of the three BCs [2]. It models the behavior of materials that are partially absorbent. Consequently, prediction of the acoustic pressure in any domain of interest requires the knowledge of the impedance at its absorbent boundaries. For a large domain, scanning the boundaries manually would be both time consuming and prone to error. In the remainder of this paper, we propose an alternative approach for this problem using a team of mobile robots based on the Two-microphone Reflection Method (TRM).

The TRM uses the phase difference between two adjacent points of a planar wave reaching the surface of the sample to measure its impedance [13]. Figure 1 shows the basic equipment setup that this method uses. Two identical, omnidirectional microphones are placed side by side in front of the sample at the desired measurement location. We denote by d_1 , d_2 , and l , the distance between the surface of the sample and the first microphone, the distance between two microphones, and the distance between the sample and the speaker, respectively.

Given a frequency $\omega = 2\pi f$ where f is in Hertz, let $p_i(\omega)$ and $p_r(\omega)$ denote incident and reflected pressure from the surface of the sample in the frequency domain. Assuming that l is large enough, the incident and reflected waves are planar. Then, the pressure readings from microphones are given by

$$\begin{aligned} p_1(\omega) &= p_i(\omega)e^{jk d_1} + p_r(\omega)e^{-jk d_1}, \\ p_2(\omega) &= p_i(\omega)e^{jk(d_1+d_2)} + p_r(\omega)e^{-jk(d_1+d_2)}, \end{aligned}$$

where $k = 2\pi/\lambda$ is the wavenumber.

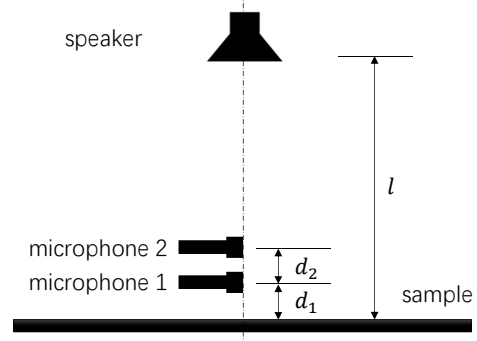


Fig. 1: Experimental setup for two-microphone reflection method.

Given measurements of $p_1(\omega)$ and $p_2(\omega)$, we can calculate the values $p_i(\omega)$ and $p_r(\omega)$. Then, the reflection coefficient is given by

$$\begin{aligned} r(\omega) &= \frac{p_r(\omega)}{p_i(\omega)} = \frac{p_2(\omega) - p_1(\omega)e^{jk d_2}}{p_1(\omega)e^{-jk d_2} - p_2(\omega)} e^{2jk d_1} \\ &= \frac{1 - H_{12}(\omega)e^{jk d_2}}{H_{12}(\omega)e^{-jk d_2} - 1} e^{2jk d_1}, \end{aligned} \quad (1)$$

where $H_{12}(\omega) = p_1(\omega)/p_2(\omega)$ is the transfer function between the microphones. Moreover, the normal surface impedance is given by

$$\begin{aligned} Z(\omega) &= \rho c \frac{1 + r(\omega)}{1 - r(\omega)} \\ &= \rho c \frac{H_{12}(\omega)(1 - e^{2jk(d_1+d_2)}) - e^{jk d_2}(1 - e^{2jk d_1})}{H_{12}(\omega)(1 + e^{2jk(d_1+d_2)}) - e^{jk d_2}(1 + e^{2jk d_1})}, \end{aligned} \quad (2)$$

where ρ and c are the density and sound speed in the medium. Often, the normalized impedance $z(\omega) = Z(\omega)/\rho c$ is used. Finally, the absorption coefficient is defined as

$$\alpha(\omega) = 1 - r^2(\omega). \quad (3)$$

Remark 2.1: The TRM has an upper bound on the frequency after which the wavelength is comparable to the size of the microphones and interference causes error in the estimations. Furthermore, the distance l between the speaker and the sample is lower bounded making compact sensor design difficult.

III. OPTIMAL PLANNING FOR MOBILE ROBOTS

In this section, we discuss how to adapt the TRM to a team of mobile robots for Autonomous Impedance Mapping (AIM) of the boundaries of a given domain \mathcal{W} , denoted by $\partial\mathcal{W}$. Specifically, we equip each robot with a speaker, two microphones, a data acquisition module, and an on-board computer that controls the robot and its communications and processes the data collected by the microphones. The microphones and speaker should maintain a minimum distance from the body of the robot to minimize acoustic interference and avoid blocking the vision sensor on the robot. A study of the design parameters is given in Section IV-B. Figure 2 shows the final design used here.

Prior to AIM, the robots map the domain \mathcal{W} and segment the boundaries $\partial\mathcal{W}$ into samples made of the same material. In order to measure the impedance of each sample, they



Fig. 2: Mobile robot equipped with a speaker and a pair of microphones.

team up in pairs of two robots which take on the roles of a speaker and listener. These teams are formed and broken up during the AIM task. The robots need to communicate to ensure that they simultaneously play the white noise and record the pressure measurements. The underlying planning problem requires scheduling the robot roles (play or record) and their positions in the domain given a set of samples to measure their impedance. As such, it can be formulated using formal languages, specifically, Linear Temporal Logic (LTL).

In order to solve the planning problem, we decompose the domain \mathcal{W} into W disjoint regions ℓ_e that can be of any arbitrary shape and may or may not contain a sample. An example of such decomposition is given in Figure 3. Next, given the robot dynamics, robot mobility in the workspace \mathcal{W} can be represented by a weighted Transition System (wTS). The wTS for robot i is defined as follows:

Definition 3.1 (wTS): A *weighted Transition System* (wTS) for a robot i , denoted by wTS_i is a tuple $\text{wTS}_i = (Q_i, q_i^0, \rightarrow_i, w_i, \mathcal{AP}_i, L_i)$ where: (a) $Q_i = \bigcup_{e=1}^W \{\{\ell_e, \text{null}\}, \{\ell_e, \text{rec}\}, \{\ell_e, \text{play}\}\}$ is the set of states, where a state (ℓ_e, act_i) indicates that robot i is at region ℓ_e and takes action act_i . The available actions are $\text{act}_i = \text{null}$ (no action), $\text{act}_i = \text{rec}$ (record sound), and $\text{act}_i = \text{play}$ (play white noise); (b) $q_i^0 \in Q_i$ collects the initial state of robot i ; (c) $\rightarrow_i \subseteq Q_i \times Q_i$ is the transition relation for robot i . Given the robot dynamics, if there exists a control input \mathbf{u}_i that can drive robot i from region ℓ_e to ℓ_k , then there is a transition from state (ℓ_e, act_i) to (ℓ_k, act'_i) for all actions act_i and act'_i ; (d) $w_i : Q_i \times Q_i \rightarrow \mathbb{R}_+$ is a cost function that assigns weights/costs to each possible transition in wTS. (e) $\mathcal{AP}_i = \bigcup_{e=1}^W \{\pi_i^{\ell_e, \text{null}}, \pi_i^{\ell_e, \text{rec}}, \pi_i^{\ell_e, \text{play}}\}$ is a set of atomic propositions, where (i) $\pi_i^{\ell_e, \text{null}}$ is true if robot i is inside region ℓ_e and takes no action, and false otherwise, (ii) $\pi_i^{\ell_e, \text{rec}}$ is true if robot i is inside region ℓ_e and records sound, and false otherwise, and (iii) $\pi_i^{\ell_e, \text{play}}$ is true if robot i is inside region ℓ_e and plays white noise, and false otherwise; and (f) $L_i : Q_i \rightarrow \mathcal{AP}_i$ is an observation/output function that returns the atomic propositions that are satisfied at state (ℓ_e, act_i) .

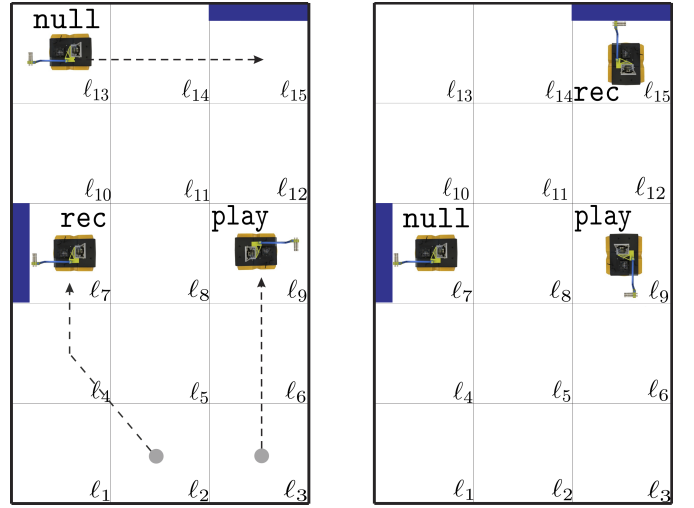


Fig. 3: Decomposition of the domain of interest \mathcal{W} into cells ℓ_e . The robots solve a planning problem that designs motion and action plans for all of them to measure the impedance of all samples while minimizing a cost function. In doing so, the robots team up in pairs of two and implement Algorithm 1. The gray dots denote the initial positions of the robots and the blue rectangles denote the samples. The figure shows the network at two time instances corresponding to impedance measurement at the two samples.

The cost function w_i in Definition 3.1 is defined as follows

$$w_i((\ell_e, \text{act}_i), (\ell_k, \text{act}'_i)) = \begin{cases} c(\ell_e, \ell_k) + \xi, & \text{if } \text{act}'_i \neq \text{null}, \\ c(\ell_e, \ell_k), & \text{o.w.,} \end{cases} \quad (4)$$

for all robots i , where $c(\ell_e, \ell_k)$ captures the distance between regions ℓ_e and ℓ_k and the robot incurs an extra cost $\xi > 0$ if it takes an action at location ℓ_k .

The AIM task, described in Section II, can be captured by the following LTL formula [14] that is defined over $2^{\cup_i \mathcal{AP}_i}$:

$$\phi = [\bigwedge_m (\diamond \phi_m)] \wedge [\square (\neg \phi_{\text{col}})] \wedge [\square (\neg \phi_{\text{obs}})] \quad (5)$$

where \diamond and \square stand for temporal operators ‘eventually’ and ‘always’, respectively [14]. In words, (5) requires the formula ϕ_m to be eventually satisfied for all samples m and the formula ϕ_{col} to never be satisfied. The (Boolean) formula ϕ_{col} is true if two or more robots are in the same region, and false, otherwise. The (Boolean) formula ϕ_{obs} is true if any robot hits an obstacle. Finally, the formula ϕ_m is defined as follows

$$\phi_m = \underbrace{(\bigvee_i \pi_i^{\ell_m, \text{rec}})}_{(a)} \wedge \underbrace{(\bigvee_{\ell_e \in \mathcal{L}_m} (\bigvee_i \pi_i^{\ell_e, \text{play}}))}_{(b)}. \quad (6)$$

In (6), part (a) requires that at least one of the robots be present at location ℓ_m , where a sample is located, and record sound. Also, part (b) requires that at least one of the robots to be present at one of the locations $\ell_e \in \mathcal{L}_m$ and play white noise, where \mathcal{L}_m is a set that collects all locations ℓ_e that satisfy the following two requirements. First, ℓ_e is within the distance $[l_{\min}, l_{\max}]$ from ℓ_m , and second there exists a point inside location ℓ_e so that the line that connects this point to the sample at ℓ_m is perpendicular to the sample surface located in ℓ_m and it is obstacle-free and there are no other robots along this line. Note that satisfaction of the second requirement ensures that at most one team of robots is assigned to each sample.

Algorithm 1 Autonomous Impedance Mapping

Require: Construct a map of the domain \mathcal{W} and segment its boundaries $\partial\mathcal{W}$ into samples;

Require: Decompose \mathcal{W} into W cells;

- 1: Construct wTS_{*i*} for all robots;
 - 2: Design plans τ_i as per the solution to problem (8);
 - 3: **for** $\kappa = 1 : \infty$ **do**
 - 4: **if** $\tau_i(\kappa) = (\ell_m, \text{rec})$ **then**
 - 5: Position the microphones with distance d_1 from the sample in cell ℓ_m ;
 - 6: Collect pressure measurements $\hat{p}_1(t)$ and $\hat{p}_2(t)$ and take the Fourier Transform to get $p_1(\omega)$ and $p_2(\omega)$;
 - 7: Calculates the transfer function $H_{12}(\omega)$ and the impedance using equation (2);
 - 8: Communicate the estimate to the network;
 - 9: **end if**
 - 10: **if** $\tau_i(\kappa) = (\ell_e, \text{play})$ **then**
 - 11: Position oneself in front of the sample;
 - 12: Play white noise;
 - 13: **end if**
 - 14: **end for**
-

Given the wTS_{*i*}, for all robots *i*, and the LTL formula (5), the goal is to synthesize motion plans τ_i , for all *i*, whose execution satisfies the global LTL formula (5). Typically, such motion plans are infinite paths in wTS_{*i*} [14], i.e., infinite sequences of states in wTS_{*i*}, such that $\tau_i(1) = q_i^0$, $\tau_i(\kappa) \in \mathcal{Q}_i$, and $(\tau_i(\kappa), \tau_i(\kappa + 1)) \in \rightarrow_i, \forall \kappa \in \mathbb{N}_+$. In this form, they cannot be manipulated in practice. This issue can be resolved by representing these plans in a prefix-suffix form, i.e., $\tau_i = \tau_i^{\text{pre}} [\tau_i^{\text{suf}}]^\omega$, where the prefix part τ_i^{pre} and suffix part τ_i^{suf} are both finite paths in wTS_{*i*}, for all robots *i*. The prefix τ_i^{pre} is executed once and the suffix τ_i^{suf} is repeated indefinitely. The cost associated with a plan $\tau_i = \tau_i^{\text{pre}} [\tau_i^{\text{suf}}]^\omega$ is defined as

$$J_p(\tau_i) = \beta J(\tau_i^{\text{pre}}) + (1 - \beta) J(\tau_i^{\text{suf}}), \quad (7)$$

where $J(\tau_i^{\text{pre}})$ and $J(\tau_i^{\text{suf}})$ represent the cost of the prefix and suffix parts, respectively, and $\beta \in [0, 1]$ is a user-specified parameter. The cost $J(\tau_i^{\text{pre}})$ of the prefix part is defined as $J(\tau_i^{\text{pre}}) = \sum_{\kappa=1}^{|\tau_i^{\text{pre}}|-1} w_i(\tau_i^{\text{pre}}(\kappa), \tau_i^{\text{pre}}(\kappa+1))$, where $|\tau_i^{\text{pre}}|$ stands for the number of states in the finite path τ_i^{pre} , $\tau_i^{\text{pre}}(\kappa)$ denotes the κ -th state in τ_i^{pre} , and w_i are the weights defined in Definition 3.1. The cost $J(\tau_i^{\text{suf}})$ of the suffix part is defined accordingly. In words, the cost function (7) captures the total distance traveled by all robots and total number of ‘record’ and ‘play’ actions taken by all robots. Given the objective (7), the planning optimization problem that we consider in this paper can be summarized as

$$\begin{aligned} \min_{\tau} \sum_{i=1}^N J_p(\tau_i) \\ \text{s.t. } \tau \models \phi, \end{aligned} \quad (8)$$

where $\tau = \otimes_{\forall i} \tau_i$ denotes the composition of all plans τ_i . Prefix-suffix motion plans τ_i that satisfy the assigned LTL task (5) and minimize the total cost $\sum_{i=1}^N J_p(\tau_i)$ can be synthesized using available optimal control synthesis algorithms under



Fig. 4: The experiment environment. Hard surfaces like wood and concrete are often modeled as fully reflective acoustic materials. Here, we place pieces of glass wool and foam on portions of the boundaries as materials whose impedance needs to be measured.

global temporal tasks [15], [16]. For the complexity analysis of the algorithm see [16, Sec. IV-D].

Algorithm 1 summarizes the actions individual robots take for AIM of the domain \mathcal{W} . Note that in line 3, τ_i is an infinite sequence of states in wTS_{*i*}, that is the reason κ goes to ∞ . Note also that in practice after a finite sequence of actions, the operation terminates. Then the plan is to do nothing without incurring any cost. Line 4 ensures that the listener robot is positioned in the relevant cell ℓ_m according to the specifications of the TRM and its action is to ‘record’. In line 6, the listener collects a time series of pressure readings $\hat{p}_1(t)$ and $\hat{p}_2(t)$ next to the sample and uses the Fourier transform to extract frequency data from this time series. Finally, line 10 checks that the speaker is positioned in the relevant cell ℓ_e with a distance l and perpendicular to the sample, cf. Figure 1, and its action is ‘play’. Note that by construction of the plans, the speaker always plays white noise while the corresponding listener is recording.

IV. EXPERIMENTAL RESULTS

In this section, we present experimental results to demonstrate the performance of the Autonomous Impedance Mapping (AIM) Algorithm 1. Particularly, we run an experiment in a non-convex environment shown in Figure 4. For highly reflective materials, e.g., concrete and wood, often a fully reflective BC suffices. Therefore, of particular interest are more absorbent materials in the domain. For the experiment, we place two pieces of glass wool and Polyurethane foam with dimensions of 24in×24in and the thickness of 1in next to the walls. These are the absorbent portions of the boundaries. Note that modern buildings are often acoustically designed using such absorbent materials. Similar materials are also used in the relevant literature [13].

We compare our results to reference estimations that we obtain using the Standing-wave Tube Method (STM). This method is based on the measurements of the ratio of magnitudes of the maximum to minimum sound pressures of the standing wave that is formed inside the tube after reflection from a desired sample [17]. The structure of the tube used here is shown in Figure 5. As mentioned earlier, acoustic properties are problem-dependent. This means that the values returned by the STM do not necessarily represent the ground truth and are only used here as a reference. We define the estimation error



Fig. 5: Tube used in the STM to generate the reference impedance values. The sample is cut to precision and placed at the end of the tube. Then, a speaker, placed in the box, plays white noise. The wave reflected from the sample creates a standing wave in the tube. Then, the ratio of the maximum to minimum pressures is used to determine the impedance of the sample.

for a given sample as the average discrepancy between the estimates returned by our method and the STM:

$$\text{err}[z] = \frac{1}{n} \sum_{i=1}^n |z(f_i) - \hat{z}(f_i)|, \quad (9)$$

where f_i is the frequency, $z(f_i)$ denotes the filtered impedance returned by the AIM algorithm, and $\hat{z}(f_i)$ is the reference value measured by the STM. Similar expressions are used for reflection and absorption coefficients. We use a low-pass filter on our data to smooth out the oscillations. Particularly, we utilize the Savitzky-Golay filter with window length 41 and polynomial order of 1. See [18] for more details.

We use two 0.5in omni-directional microphones on each robot and set the distance between the sample and first microphone to $d_1 = 12\text{mm}$, the distance between microphones to $d_2 = 16\text{mm}$, and the distance between the speaker and the sample to $l = 1.2\text{m}$. Note that these are the optimal design parameters obtained through a parameter study that is presented in Section IV-B. A distance range of $l \in [1.1, 1.4]$ between the listener and speaker pairs works well in practice.

A. Autonomous Impedance Measurements

In this section, we discuss the construction of the Impedance Map (IM) for the domain in Figure 4 using two mobile robots. According to Algorithm 1, the robots construct a map of the domain \mathcal{W} , decompose it into W cells, and then solve the planning optimization problem (8) to obtain a sequence of waypoints and actions that minimize the traveled distance and ensure that the AIM task is accomplished. The plan for this experiment is shown in Figure 6. The speaker does not change throughout the experiment. It places itself in the intersection of the two samples and performs two ‘play’ actions in accordance with the listener that moves from glass wool to foam, sequentially. For the decomposition of the domain shown in Figure 6, the available motion actions are up, down, left, right, up and left, up and right, down and left, down and right, and stay idle. The plans for the two robots that satisfy (5), computed as per [16], are as follows:

$$\begin{aligned} \tau_1 &= (\ell_1, \text{null})(\ell_4, \text{rec})(\ell_8, \text{null})(\ell_{12}, \text{rec})[(\ell_{12}, \text{null})]^\omega, \\ \tau_2 &= (\ell_3, \text{null})(\ell_6, \text{play})(\ell_6, \text{null})(\ell_6, \text{play})[(\ell_6, \text{null})]^\omega. \end{aligned}$$

The robots construct the IM during the implementation of the prefix part of the plan; cf. Section III. Specifically, they collect pressure measurements of the glass wool at step $\kappa = 2$ and the foam at step $\kappa = 4$. The suffix part of the plan ensures

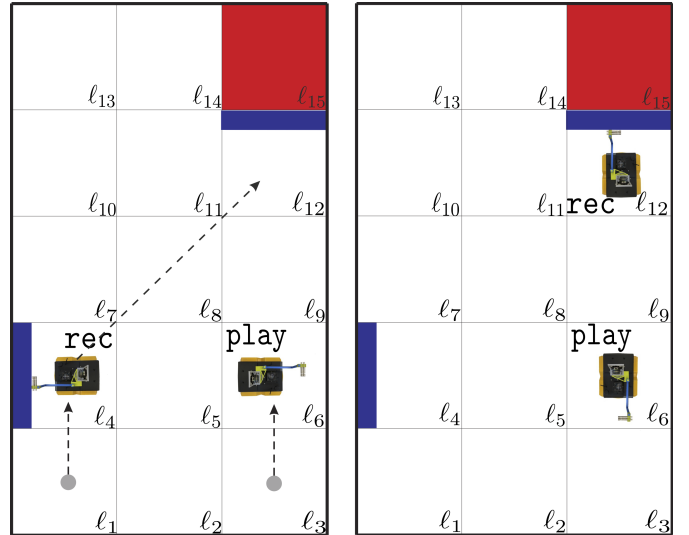


Fig. 6: Plan constructed by robots by solving the planning problem (8) for the experiment. The robots implement Algorithm 1 to construct the desired IM for the boundaries of the domain. The left and right figures correspond to steps $\kappa = 2$ and $\kappa = 4$ of the plan, respectively. Location ℓ_{15} corresponds to an obstacle in the workspace that should always be avoided.

TABLE I: Error values (9) in estimation of acoustic properties.

sample	reflection	impedance	absorption
glass wool	0.034	0.15	0.011
foam	0.050	0.17	0.021

that the robots do not incur any extra costs. See [19] for an animation of this experiment.

Figure 7a shows the estimates of the complex normalized impedance values for glass wool for a frequency range of 1–4kHz. Figure 7b shows similar data for Polyurethane foam but for a shorter frequency range of 1–2.6kHz. This is because the impedance values deviate from that of the STM in a smaller frequency in the latter case. In practice the intersection of these two frequency ranges should be used so that the IM for all boundary segments are available. Note that our data shows an upper frequency that is almost double in magnitude compared to [13]. The error values are reported in Table I. All values are normalized and dimensionless. The error values are larger for impedance since the magnitude of impedance is not bounded in $[0, 1]$. Note that the minimum frequency for the STM is determined by the size of the tube and is limited to 700Hz for the one used here, cf. Figure 5. On the other hand, the largest frequency for the TRM is bounded by the wavelengths that are comparable to the size of microphones; cf. Remark 2.1.

B. Design Parameters

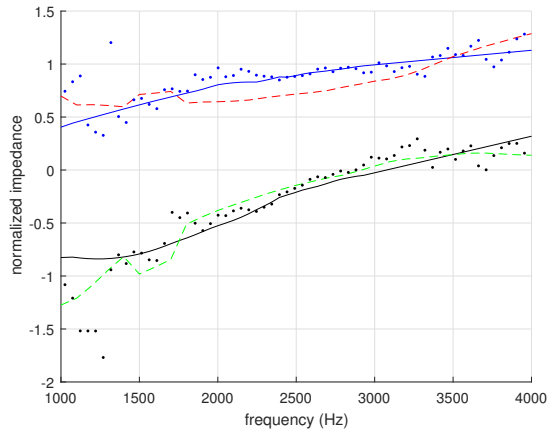
The structure of the mobile robots and the arrangement of the sensors and the speaker on them affect the accuracy of the experimental results. Specifically, our experiments indicate that the lowest impedance error values are obtained for the smallest values of d_1 and d_2 . Note that, the minimum value of d_1 is limited by the accuracy of the motion control and the minimum value of d_2 is limited by the diameter of the microphones. We use $d_1 = 12\text{mm}$ and $d_2 = 16\text{mm}$ in the experiments. Figure 8 shows the impedance error as a function

V. CONCLUSION

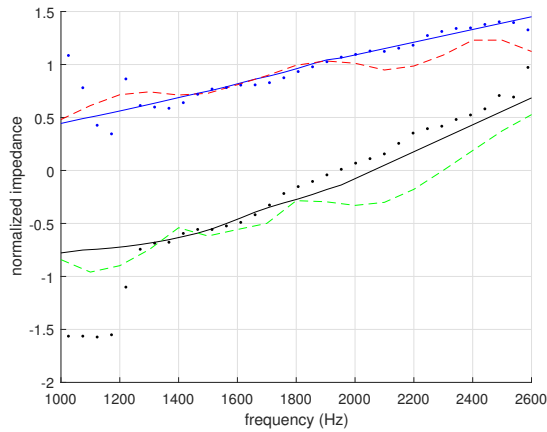
In this paper we addressed the problem of Autonomous Impedance Mapping (AIM) of an environment using a team of mobile robots. Particularly, we utilized the two-microphone reflection method to estimate the normal surface impedance of the boundaries. We modeled the proposed collaborative AIM task using Linear Temporal Logic and addressed its solution. Finally, we presented experimental results in which we validated our impedance measurements by comparing to the standing-wave tube method.

REFERENCES

- [1] M. Moser, *Engineering Acoustics: An Introduction to Noise Control*. Springer, 2004.
- [2] A. B. C. Lawrence E. Kinsler, Austin R. Frey and J. V. Sanders, "Fundamentals of acoustics," 1982.
- [3] L. Calkins, R. Khodayi-mehr, W. Aquino, and M. Zavlanos, "Stochastic model-based source identification," in *Proceedings of IEEE Conference on Decision and Control*, pp. 1272–1277, 2017.
- [4] R. Khodayi-mehr, W. Aquino, and M. M. Zavlanos, "Distributed reduced order source identification," in *Proceedings of American Control Conference*, pp. 1084–1089, June 2018.
- [5] R. Khodayi-mehr, W. Aquino, and M. M. Zavlanos, "Model-based active source identification in complex environments," *IEEE Transactions on Robotics*, 2018. (accepted). [Online]. Available: <https://arxiv.org/pdf/1706.01603.pdf>.
- [6] M. Garai, "Measurement of the sound-absorption coefficient in situ: the reflection method using periodic pseudo-random sequences of maximum length," *Applied Acoustics*, vol. 39, no. 1-2, pp. 119–139, 1993.
- [7] International Organization for Standardization, *ISO 354-2003 Acoustics — Measurement of sound absorption in a reverberation room*.
- [8] W. O. Hughes, A. M. McNelis, C. Nottoli, and E. Wolfram, "Examination of the measurement of absorption using the reverberant room method for highly absorptive acoustic foam," 2015.
- [9] A. Farina and P. Fausti, "Standing wave tube techniques for measuring the normal incidence absorption coefficient: comparison of different experimental setups," in *Proceedings of International FASE Symposium*, 1994.
- [10] J. Chung and D. Blaser, "Transfer function method of measuring induct acoustic properties. II. experiment," *The Journal of the Acoustical Society of America*, vol. 68, no. 3, pp. 914–921, 1980.
- [11] H. Utsuno, T. Tanaka, T. Fujikawa, and A. Seybert, "Transfer function method for measuring characteristic impedance and propagation constant of porous materials," *The Journal of the Acoustical Society of America*, vol. 86, no. 2, pp. 637–643, 1989.
- [12] J. F. Allard and B. Sieben, "Measurements of acoustic impedance in a free field with two microphones and a spectrum analyzer," *The Journal of the Acoustical Society of America*, vol. 77, no. 4, pp. 1617–1618, 1985.
- [13] Y. Takahashi, T. Otsuru, and R. Tomiku, "In situ measurements of surface impedance and absorption coefficients of porous materials using two microphones and ambient noise," *Applied Acoustics*, vol. 66, no. 7, pp. 845–865, 2005.
- [14] C. Baier and J.-P. Katoen, *Principles of model checking*, vol. 26202649. MIT press Cambridge, 2008.
- [15] A. Ulusoy, S. L. Smith, X. C. Ding, C. Belta, and D. Rus, "Optimality and robustness in multi-robot path planning with temporal logic constraints," *The International Journal of Robotics Research*, vol. 32, no. 8, pp. 889–911, 2013.
- [16] Y. Kantaros and M. M. Zavlanos, "Sampling-based optimal control synthesis for multi-robot systems under global temporal tasks," *IEEE Transactions on Automatic Control*, 2018.
- [17] International Organization for Standardization, *ISO 10534-1 Acoustics — determination of sound absorption coefficient and impedance in impedance tubes. Part 1: method using standing wave ratio*.
- [18] A. Savitzky and M. J. Golay, "Smoothing and differentiation of data by simplified least squares procedures," *Analytical Chemistry*, vol. 36, no. 8, pp. 1627–1639, 1964.
- [19] "Animation - <https://vimeo.com/290174082>."



(a) glass wool



(b) Polyurethane foam

Fig. 7: Normalized impedance values for glass wool and Polyurethane foam. The dots show data points and the solid lines are the corresponding filtered data. The dashed lines show the estimates from STM.

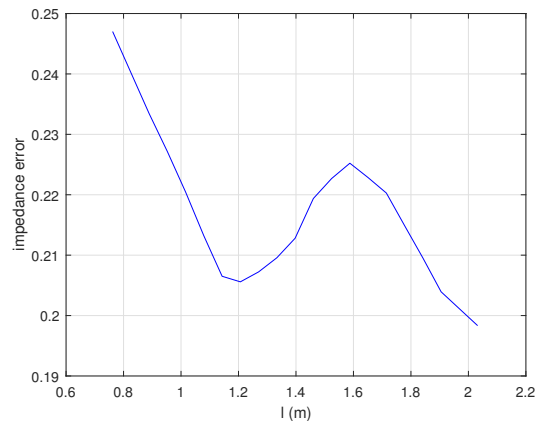


Fig. 8: Impedance error versus the distance between the sample and speaker.

of the distance l between the sample and speaker. The first minimum error occurs around $l = 1.2$ which is the distance used in our experiments.